COMMUNICATION

Probing the Local Conformation within π-Conjugated One-dimensional Supramolecular Stacks using Frequency Modulation Atomic Force Microscopy

By *Benjamin Grévin,* Renaud Demadrille, Mathieu Linares, Roberto Lazzaroni,* and *Philippe Leclère**

Frequency modulation atomic force microscopy is used to investigate the local conformation within 1D stacks obtained by the self-assembly of π-conjugated molecules from solution. These 'molecular wires' are formed of π-stacked dioctylquaterthiophene-substituted fluorenone molecules, adsorbed in an 'edge-on' configuration. Several conformers coexist within the supramolecular assemblies, as revealed by high-resolution topographic and dissipation images acquired for the first time in the non-contact regime. The structural parameters (in particular the width and height of the stacks) extracted from the experimental data can be interpreted in terms of local molecular conformation, by comparison with models obtained by molecular mechanics and dynamics simulations. Upon in-situ annealing, a molecular reorganization towards the most stable conformation occurs within the assemblies, which leads to highly regular arrays of nanowires. These results represent a significant advance in the understanding of the internal structure and dynamics of solid-state π-conjugated assemblies and open novel perspectives for local investigations of self-assembled nanostructures.

Near-field microscopy techniques appear to be essential tools for fundamental and technological research in the field of organic and molecular electronics. A detailed understanding of the molecular conformation, self-organization, and electronic properties on surfaces is indeed required for the optimization of electronic and optoelectronic devices such as organic field-effect transistors (OFETs),[1–4] organic light-emitting diodes (OLEDs),[5] photovoltaic cells,[6–9] or sensors.[10]

Because 1D systems are the structures with the lowest dimension that permit efficient electron transport, nanowires are expected to be critical for nanometer-scale electronic devices. At present, a wide range of materials that range from metals and inorganic semiconductors to carbon nanotubes have been fabricated into nanowires.[11] In this context, the fabrication of 1D structures from molecular systems is a most important step to generate organic nanometer-scale electronic devices. Such 'molecular nanowires' can be formed by π-stacking of conjugated molecules or polymer chains adsorbed 'edge-on' on the substrate surface. Those structures, which are often formed from solution, show higher field-effect mobility with respect to homogenenous films[11,12] or better performances in organic photovoltaic devices.[13]

While scanning tunneling microscopy is extremely powerful for investigating 'face on' molecular layers,[14–18] it is rarely applicable to 'edge on' functional supramolecular assemblies, and is restricted to conducting surfaces. Atomic force microscopy (AFM) constitutes a more universal approach and has been widely applied in ambient conditions in intermittent contact (also called amplitude modulation mode, AM-AFM) to characterize the microscopic morphology of solution-processed π-conjugated oligomers and polymers deposited in thin films on conducting and insulating surfaces,[19–22] such as the substrates used for the gate dielectric in OFETs. The resolution achieved by AFM is typically a few nanometers. The technique can provide valuable information on the size and shape of the nanostructures in ambient conditions. However, the exact nature of the molecular packing within functional π-conjugated assemblies often remains unknown, because of the limits in spatial resolution of AFM in the amplitude modulation mode. For instance, images reveal the fibrillar organization of the stacks[19–22] but provide no information on their internal structure.

Non-contact AFM (NC-AFM) in ultra-high vacuum (UHV) in the frequency modulation mode (FM-AFM)[23,24] provides a higher resolution, and could, therefore, yield an improved description of the structure of the π-conjugated nanowires. Over the past few years, monolayers and single molecules have been investigated by NC-AFM on conducting[25] and insulating surfaces,[26] and sub-molecular resolution has been achieved in the frequency modulation mode on a few molecular single crystals.[27] So far, to the best of our knowledge, no NC-AFM investigation has been reported on solution-processed 1D π-conjugated nanostructures.

In this context, here we use NC-AFM in UHV in the frequency modulation mode to obtain information with unprecedented resolution on the molecular conformation within π-conjugated supramolecular assemblies. We have investigated the self-

[*] Dr. B. Grévin, Dr. R. Demadrille
Laboratoire d'Electronique Moléculaire Organique et Hybride (LEMOH)
UMR5819-SPrAM (CEA-CNRS-University Grenoble I)
INAC CEA-Grenoble, 38054
Grenoble Cedex 9 (France)
E-mail: benjamin.grevin@cea.fr
Dr. P. Leclère, Dr. M. Linares, Prof. R. Lazzaroni
Service de Chimie des Matériaux Nouveaux
Université de Mons-Hainaut
Mons, 7000 (Belgium)
E-mail: philippe.leclere@umh.ac.be
Dr. M. Linares
Department of Physics, Chemistry and Biology
Linköping University
58183 Linköping (Sweden)

DOI: 10.1002/adma.200803762

ADVANCED MATERIALS

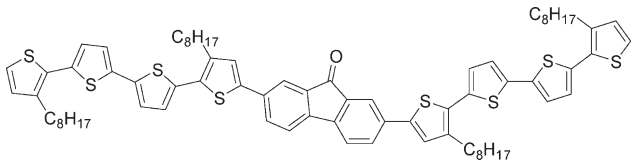

Scheme 1. Chemical structure of QTF8.

assembly of a conjugated oligomer made of two octyl-substituted quaterthiophene segments attached to a central fluorenone unit, namely (2,7-bis-(3,3‴-dioctyl-[2,2′;5′,2″;5″,2‴]quaterthiophen-5-yl)-fluoren-9-one (QTF8) (Scheme 1).[28] The identification of the different conformers involved in the supramolecular stacks has been achieved by combining high-resolution topographic and dissipation imaging, with the results of molecular mechanics (MM) and molecular dynamics (MD) simulations.

The QTF8 molecule consists of a fluorenone central unit symmetrically coupled to two quaterthiophene segments. The alkylated quaterthiophene building blocks provide optical absorption in the visible spectrum and hole-carrier properties to the final system, and are symmetrically coupled to the fluorenone central unit, which allows a fine-tuning of the optical and redox properties and gives a donor–acceptor molecular system well-adapted for application as the active component of the bulk heterojunction with PCBM-C_{60}.[28] The presence of multiple alkyl chains promotes the solubilization of the molecule in various solvents. When QTF8 is deposited by drop casting from a dilute anhydrous toluene solution on a variety of substrates such as mica, SiO_2, or Al_2O_3, the molecules spontaneously form ordered aggregates. When QTF8 is deposited on freshly cleaved, highly oriented pyrolytic graphite (HOPG) substrates, AM-AFM images in ambient conditions reveal that the thin deposits are formed by stacks or fibrils, with an effective height of ~3 nm (Fig. 1 and Fig. S1 in the Supporting Information). The formation of thin deposits has been studied for series of similar oligomers,[29,30] which revealed that the self-assembly at surfaces is mainly governed by the molecule–molecule (or inter-segment) interactions and the molecule–substrate interactions, and leads to well-defined nanostructures, either 2D ultrathin regular layers or 1D fibrillar objects.

Considering the size of the QTF8 molecule (about 4 nm long, 2.5 nm wide, and 0.5 nm thick in its fully planar conformation), the value for the stack height clearly suggests that these molecular aggregates are formed of π-stacked oligomers in the 'edge-on' configuration, in which the plane of the conjugated system is perpendicular to the substrate and with fully extended octyl groups. This is somewhat striking, as one may expect a relatively strong interaction of the π-system and the alkyl substituents with the underlying graphite surface, which would give rise to the formation of 'face-on' 2D assemblies instead of 'edge-on' stacks. It appears that the 'edge-on' molecules are in fact deposited over a monolayer of 'face-on' molecules, as shown by FM-AFM images presented later (Fig. 4 and Fig. S6 in the Supporting Information). This monolayer of 'face-on' molecules acts as a buffer layer for the formation of the 'edge-on' supramolecular stacks, and strongly attenuates the influence of the substrate on their nanostructure. The detailed discussion of the self-assembly of this first layer is beyond the scope of this letter and will be presented in a forthcoming paper.

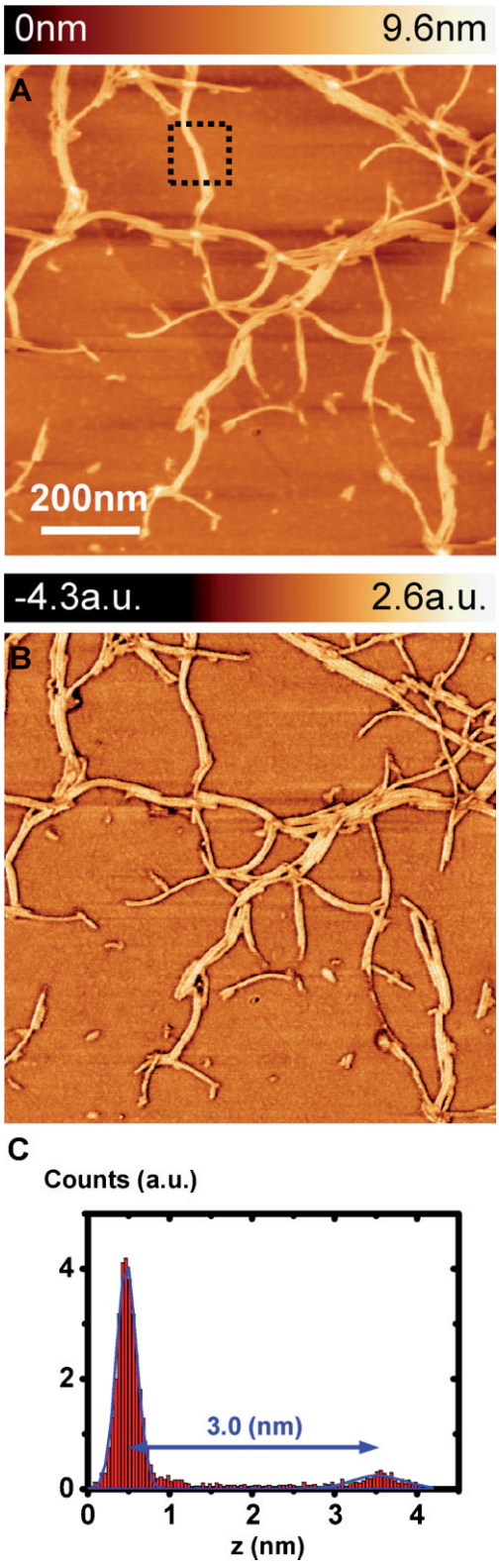

Figure 1. A,B) AM-AFM topographic and phase images (in ambient conditions) of a QTF8 deposit on HOPG. Scan size: 1.0 μm × 1.0 μm; C) Height histogram extracted from the area delimited by dotted square in the image A).

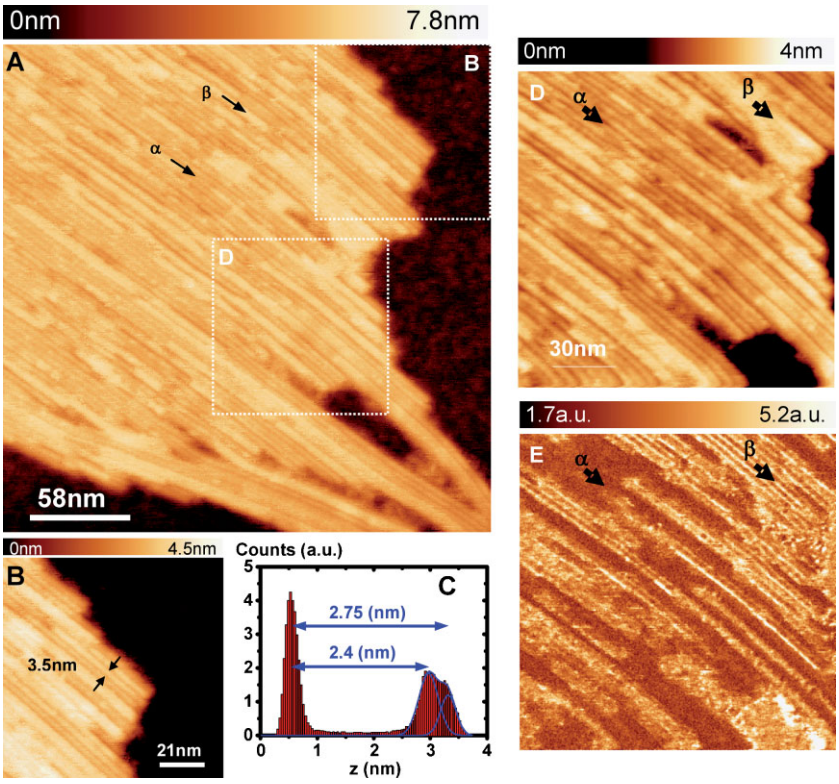

Figure 2. FM-AFM (UHV, 300 K) topographic image (scan size: $292 \times 292\,nm^2$, 730×730 pixels) of a QTF8 sample on HOPG ($\Delta f = -38$ Hz, $A_{vib} = 8.4$ nm). B) $105 \times 105\,nm^2$ digital zoom extracted from image (A). The periodic lateral distance (average value from different images) is 3.5 ± 0.2 nm. C) Histogram of the height values from image (B), which indicates the presence of two topographic levels (α and β): $\alpha = 2.4 \pm 0.1$ nm, $\beta = 2.75 \pm 0.1$ nm. Topographic (D) and dissipation (E) FM-AFM images (150 nm × 150 nm, 750 × 750 pixels) of the QTF8 deposit ($\Delta f = -38$ Hz, $A_{vib} = 8.4$ nm). The contrast in the dissipation image shows a one-to-one correspondence with the variations in the height levels in the topographic image, as highlighted by the black arrows.

To gain a deeper insight on the molecular organization within the stacks, FM-AFM investigations were conducted and their results were interpreted with the assistance of molecular modeling simulations. The FM-AFM data (Fig. 2A–E) reveal that the molecular assemblies are composed of close-packed nanowires that lie side-by-side. Two levels of topographic elevation can be detected, designated by α and β on Figure 2A. Within α domains, the nanowires are better resolved, with an apparent width of 3.5 ± 0.2 nm (the length of the fully extended molecule is 3.8 nm). As previously deduced from the AM-AFM data, the height values (2.4 nm and 2.75 nm for α and β nanowires, respectively) are consistent with the 'edge-on' arrangement of π-stacked QTF8 molecules. The two levels are interpreted as the result of local differences in the conformation of the alkyl-substituted thiophene units (see below).

From the FM-AFM topographic image, it can be clearly seen that along a given nanowire, areas appear with different colors, which correspond to segments of different heights (the darker ones being at lower elevation). These variations in height are most probably a result of local differences in the conformation of the alkyl-substituted thiophene units located along the conjugated backbone, as confirmed hereafter by molecular modeling simulations. The dissipation image in Figure 2D, which is related to the tip-sample local interaction,[23,24] clearly shows a one-to-one correspondence with the height image (Fig. 2E), a higher level of dissipation being recorded over β nanowires. We hypothesize that the way the energy brought by the oscillating tip is dissipated in the layer depends on the local molecular conformation of the stacks, in particular, the orientation of the asymmetrically substituted thiophene units. The dissipation contrast is most probably related to the degrees of freedom and flexibility of the lateral alkyl groups and π-conjugated (i.e., quaterthiophene and fluorenone) segments within the oligomer's assembly. To address more precisely this issue, one would need to develop a suited modeling formalism, which is beyond the scope of the current report.

In order to optimize the resolution of topographic images in correspondence with the dissipation contrast, a series of images was systematically recorded at the same location for different frequency shift set-points (see Supporting Information, Fig. S2), and force–spectroscopy measurements were performed to check the nature of the cantilever–sample interaction (see Supporting Information, Fig. S3). All images were acquired in the true non-contact mode, i.e., in the attractive part of the force potential curve with negative frequency shift set-points. For frequency shift set-points below approximately −10 Hz, a better resolution is achieved in the topographic images, which corresponds to the threshold of the appearance of a contrast in the dissipation images, as confirmed by the spectroscopic data (see Supporting Information, Fig. S3). All the images analyzed in this work have been acquired in the attractive regime with frequency shift set-points below −20 Hz, which ensures that the system is operating in the non-contact mode, while offering a sharper contrast between the different areas in the dissipation images.

MM and MD simulations have then been carried out in order to investigate the organization of the QTF8 molecules in the assemblies and the calculated structural parameters have been compared with the FM-AFM data. These simulations also provide information on the nature of the intermolecular interactions that govern the supramolecular organization.

We considered that the thiophene units within the two quarterthiophene segments are in an *anti*-conformation (i.e., the sulfur atoms of adjacent rings point in opposite directions), which is the most stable situation in oligo- and poly(thiophene)s. We then examined the relative orientation of the two innermost thiophene rings with respect to the fluorenone unit; they can be either in the *syn*-conformation (the sulfur atom and the C=O pointing in the same direction) or in the *anti*-conformation (the sulfur atom and the C=O pointing in opposite directions). This gives rise to three conformers (*syn–syn*, *syn–anti*, *anti–anti*), which

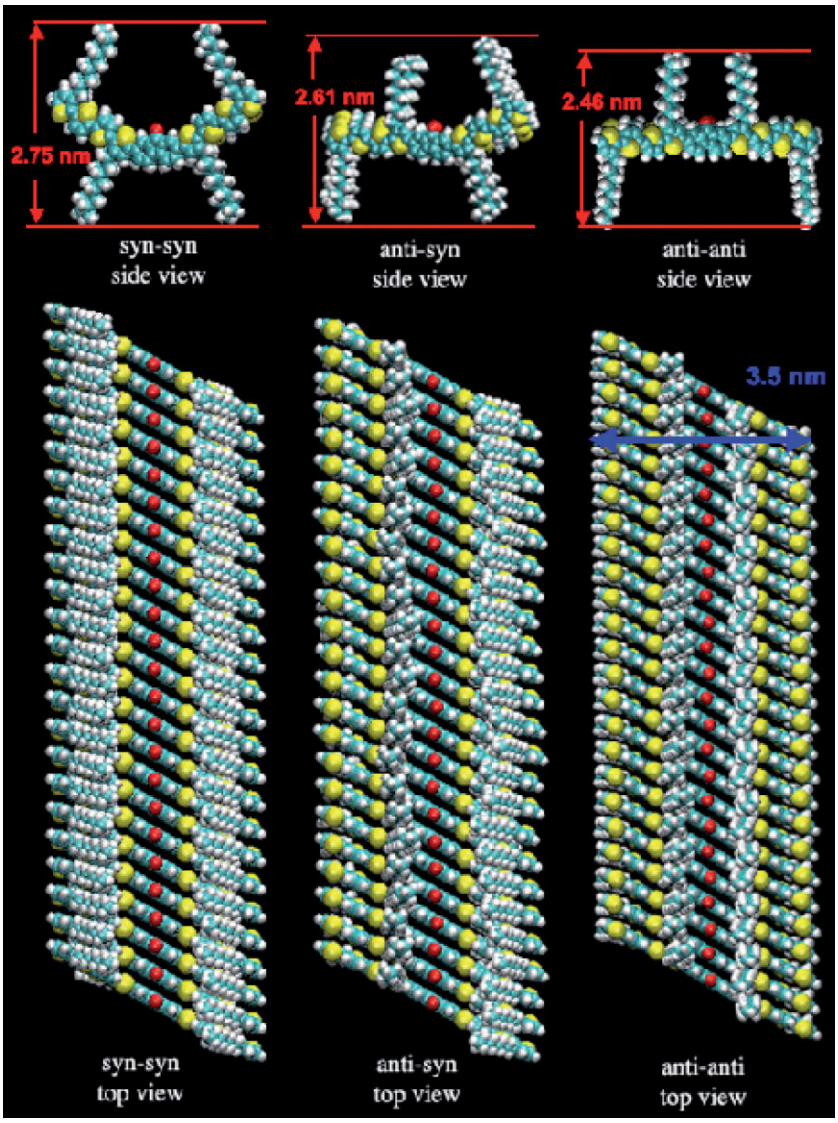

Figure 3. Molecular modeling calculations of 'edge-on' assemblies formed from QTF8 *syn–syn*, *anti–syn*, and *anti–anti* conformers (from left to right). Note that the heights of the *anti–anti* and *syn–syn* assemblies match well the two topographic levels in the histogram of Figure 4C, while their width is in excellent agreement with the lateral periodicity deduced from the experimental data (Fig. 4B and D).

are represented on top of (Fig. 3). The major geometrical difference between those conformers is the overall shape of the conjugated core, which is curved in the *syn–syn* system whereas it is straight for the *anti–anti* system. As a result, the height of the molecule is larger for the *syn–syn* conformer (2.75 nm) than for its *anti–anti* counterpart (2.46 nm). The situation in the *syn–anti* system is intermediate (2.61 nm). We observe that the heights of the two 'populations' of nanowire segments detected in the topographic images (e.g., in Fig. 2) closely match the calculated values for the *syn–syn* and the *anti–anti* conformations. This suggests that these segments are assemblies of different conformers, the majority in *anti–anti* and *syn–syn* configurations. It is difficult, however, to totally exclude the existence of *syn–anti* segments within the stacks.

In a second step, assemblies formed of 'edge-on' π-stacked molecules (in the *syn–syn*, *syn–anti*, or *anti–anti* conformation) have been modeled (see Fig. 3), with the C=O bonds of the fluorenone units all pointing in the same direction within a given wire (this configuration being more stable than the one with alternating orientation of the fluorenone units along the wire). The results of the MD calculations indicate that the molecules within the three assemblies are slightly tilted with respect to the stacking axis. This tilt corresponds to the best compromise between the maximization of the π–π interactions and the reduction of unfavorable dipole–dipole interactions. Because of this tilt, the width of the nanowires is slightly smaller than the length of the molecule (3.5 nm versus 3.8 nm), which is in excellent agreement with the value deduced from the experimental data (Figs. 2B and 4D).

The three types of π-stacked nanowires are stable, with the *anti–anti* assembly more stable than the other two systems (by about 3.5 kcal mol^{-1} per molecule), mostly because of better π–π interactions between the core of the oligomers, and a better van der Waals interaction between the alkyl chains. Control calculations show that mixed stacks, that is, stacks made of a random distribution of the three conformers, are significantly less stable than the three homogeneous stacks. At this stage, we can thus conclude that the aggregates, as formed from solution, are composed of one-molecule-wide wires that contain segments made of π-stacked molecules in a specific conformation.

Thermal or solvent annealing is known to improve the order in solid-state organic assemblies, by reducing the number of defects. Figure 4 illustrates the morphology of the stacks after a thermal annealing; both the height (Fig. 4A) and the dissipation (Fig. 4B) images are much more homogeneous. Upon annealing, the width of the nanowires becomes 7.0 ± 0.2 nm over most parts of the assembly, i.e., roughly twice the initial value.

This doubling of the lateral periodicity is well accounted for by modeling the conformation of adjacent nanowires within a 2D stack (Fig. 4C). After the annealing process, one can reasonably assume that the nanowires are mostly composed of the most stable conformers (*anti–anti*). When examining the assembly of adjacent nanowires in a 2D layer, one can consider: i) alternating the tilting angle from one stack to the next, and ii) alternating the orientation of the fluorenone units (i.e., with the C=O bond upwards or downwards) from one stack to the next. We have found that the most stable situation is with: i) non-alternating tilting and ii) an alternating orientation of the fluorenone units. This yields layers that are non-polar, because of the alternation in

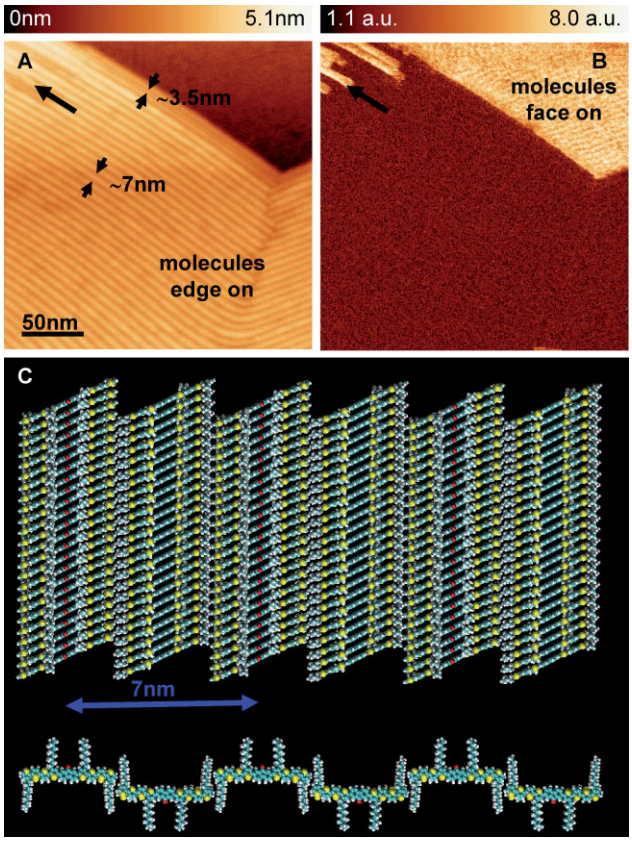

Figure 4. A) FM-AFM topographic and B) dissipation images (scan size: 250 nm × 250 nm, 1000 × 1000 pixels) of QTF8 after in-situ annealing ($\Delta F = -25.5$ Hz, $A_{vib} = 8.4$ nm). The modulation visible in the upper right corner of the dissipation image reveals the existence of a monolayer of 'face-on' QTF8 molecules, which coexists with the 'edge-on' stacks (see the Supporting Information). C) Model of the most stable 2D arrangement of stacks (top view and side view of a section). The orientation of the fluorenone units alternates from one stack to the next, which yields non-polar layers (see text), and results in a doubling of the lateral periodicity (from around 3.5 nm to around 7.0 nm), as revealed by the experimental data.

the fluorenone orientation, as illustrated by the oxygen atoms (in red) in Figure 4C. Upon optimization of these assemblies, a small displacement in the direction perpendicular to the layer occurs from one stack to the next, which improves the lateral interaction and the locking between the terminal-substituted thiophene units in adjacent nanowires (this clearly appears in the section through the layer shown in Fig. 4C). As a result, the lateral periodicity doubles, from around 3.5 nm to around 7.0 nm, which is consistent with the experimental observation.

Finally, room-temperature MD simulations have been performed in the canonical ensemble (constant *N*, *V*, *T*). The overall structure of the layer is maintained, with some slight displacements of the molecules within the stacks (see Supporting Information, Fig. S4). Fluctuating alkyl side groups point outwards, alternating with zones where the fluorenone units and unsubstituted thiophene rings are exposed. The topographic profiles extracted from high magnification images in the direction of the main modulation (see Supporting Information, Fig. S5) are in very good agreement with the shape simulated by MD.

At room temperature, the thermal fluctuations of the lateral side groups prevent more precise resolution of the local conformation at the submolecular scale. Further FM-AFM studies at low temperature (30 K) are planned to probe the local conformations at the sub-molecular scale within oligomer-based edge-on π-conjugated stacks.

The use of FM-AFM to investigate thin deposits of conjugated oligomers brings important new insight on the intimate supramolecular organization in π-conjugated assemblies on surfaces, and more specifically on the presence of local variations in the molecular conformation. Extension to other types of organic or bio-nanostructures can be expected to provide valuable information on the conformational properties on the local scale in functional self-assembled architectures.

Experimental

Synthesis of QTF8: QTF8 was prepared using a synthetic strategy [28,31] based on the Stille cross-coupling reaction between 2,7-dibromofluoren-9-one and α-stanylated 3,3‴-dioctyl-[2,2′;5′,2″;5″,2‴]-quaterthiophene, the latter being synthesized following the procedure reported by Herrema et al. [32]. All commercially available reagents were used as received without further purification. Solvents were dried and distilled prior to use. All reactions were carried out in standard glassware under an inert argon atmosphere. Merck silica gel 60 (0.063–0.200 mm) was used for column chromatography. All synthesized products were identified by ^{1}H and ^{13}C NMR spectroscopy, as well as by elemental analysis. NMR spectra were recorded in deuterated chloroform that contained tetramethylsilane as an internal standard, on a Brüker AC200 spectrometer. Elemental analyses (C and H) were carried out by the Analytical Service of the CNRS (Vernaison, France).

Sample Preparation for AFM Measurements: Thin deposits of QTF8 were prepared by drop casting 10 μL of an anhydrous toluene solution (concentration 0.05 mg · mL^{-1}) on freshly cleaved highly oriented pyrolytic graphite (HOPG) substrates. The solvent was slowly evaporated under a toluene saturated atmosphere for 24 h.

AFM Experiments: As a first stage in this work, AM-AFM measurements were performed, with a Nanoscope V microscope from Veeco (operating in air at room temperature). Microfabricated silicon cantilevers (Nanosensors) were used with a spring constant of ~30 N · m^{-1}. The purpose of the experiments was to set the proper sample preparation conditions to obtain reproducible deposits with a well-defined morphology. Based on the results, FM-AFM experiments were then carried out at room temperature in ultrahigh-vacuum conditions (5×10^{-11} mbar), using a VT-beam AFM system (optical deflection non-contact AFM) controlled by a Matrix unit from Omicron, and supersharp silicon cantilevers (Nanoworld, resonance frequency in the 260–410 kHz range). The scanner tube was calibrated by recording atomically resolved scanning tunneling microscopy images of the reconstructed Si(111)–7 × 7 surface. The cantilever vibration amplitude A_{vib} was calibrated using both a procedure provided by the SPM manufacturer for the geometry of the VT-beam AFM setup, and by a spectroscopic method. In the latter, the variation of the tip height *z* was recorded as a function of the amplitude swept step by step ($\Delta A_{vib} = A_{vib2} - A_{vib1}$), while keeping the normalized frequency shift $\gamma = \Delta f \times A_{vib}^{3/2}$ constant (by adapting the frequency detuning for each step, $\Delta f_2 \times A_{vib2}^{3/2} = \Delta f_1 \times A_{vib1}^{3/2}$). In the limit of large amplitudes, the frequency shift at constant *d* is proportional to $A_{vib}^{3/2}$, *d* being the distance between the apex of the tip and the surface at the lower turning point of the oscillation. By keeping $\Delta f \times A_{vib}^{3/2}$ constant, one gets height steps $\Delta z = \Delta A_{vib}/2$, which allows a direct estimation of the amplitude. The two calibration methods yield similar results. All FM-AFM images were acquired in the non-contact mode, i.e., in the attractive part of the force

potential curve with negative frequency shift set-points. This point was checked by performing force-spectroscopy measurements (acquisition of $\Delta f(z)$ and damping (z) curves). Two-dimensional spectroscopic data (supporting information) were acquired in a mode in which the topographic images (acquired at a fixed frequency shift) are recorded simultaneously with $\Delta f(z)$ and damping (z) curves taken on a grid, the feedback loop being disabled during spectroscopic acquisition. The sample annealing was performed in situ under UHV at 130 °C for 6 h.

AFM Image Processing: WsXM [33] software (Nanotec Electronica, Spain) has been used for AFM image processing.

Molecular Modeling: All the molecular modeling calculations have been performed with the Tinker package (http://dasher.wustl.edu/tinker) and the MM3 force-field, which is parameterized to accurately describe weak interactions such as π–π stacking [34,35]. MD simulations of the molecular assemblies on graphite have been carried out in the canonical ensemble (constant N, V, T) at 300 K, using periodic boundary conditions.

Acknowledgements

The collaboration between Grenoble and Mons has been carried out in the frame of a joint bilateral research program (FNRS-CGRI/CNRS 20182). Y. Kervella and Dr. F. Lincker are acknowledged for their help during the preparation of the QTF8 molecule. The modelling work in Mons has been supported by the European Commission Marie Curie Research Training Network CHEXTAN (MRTN-CT-2004-512161), by the Interuniversity Attraction Pole program of the Belgian Federal Science Policy Office (PAI 6/27) and by FNRS-FRFC. SPM facilities used for the experimental work within UMR5819-SPrAM have been funded by the French Ministry of Research under the grant 'RTB: Post CMOS, Moléculaire 200 mm'. Ph.L is Research Associate of the FRS-FNRS (Belgium). R.D. thanks ANR for funding through the Nanorgysol and Conaposol research programs. Supporting Information is available online from Wiley InterScience or from the author.

Received: December 19, 2008
Revised: April 28, 2009
Published online: June 8, 2009

[1] C. Reese, M. Roberts, M.-M. Ling, Z. Bao, *Mater. Today* **2004**, *7*, 20.
[2] H. Siringhaus, *Adv. Mater.* **2005**, *17*, 2411.
[3] S. Allard, M. Forster, B. Souharce, H. Thiem, U. Scherf, *Angew. Chem. Int. Ed.* **2008**, *47*, 2.
[4] a) A. R. Brown, A. Pomp, C. M. Hart, D. M. de Leeuw, *Science* **1995**, *270*, 972. b) B. Crone, A. Dodabalapur, Y. Y. Lin, R. W. Filas, Z. Bao, A. LaDuca, R. Sarpeshkar, H. E. Katz, W. Li, *Nature* **2000**, *403*, 521. c) C. J. Drury, C. M. J. Mutsaers, C. M. Hart, M. Matters, D. M. de Leeuw, *Appl. Phys. Lett.* **1998**, *73*, 108.
[5] J. H. Burroughes, D. D. C. Bradley, A. R. Brown, R. N. Marks, K. MacKay, R. H. Friend, P. L. Burnes, A. B. Holmes, *Nature* **1990**, *347*, 539.
[6] W. Ma, C. Yang, X. Gong, K. Lee, A. J. Heeger, *Adv. Funct. Mater.* **2005**, *15*, 1617.
[7] J. Y. Kim, K. Lee, N. E. Coates, D. Moses, T.-Q. Nguyen, M. Dante, A. J. Heeger, *Science* **2007**, *317*, 222.
[8] A. C. Mayer, S. R. Scully, B. E. Hardin, M. W. Rowell, M. D. McGehee, *Mater. Today* **2007**, *10*, 28.
[9] a) W. U. Huynh, J. J. Dittmer, W. C. Libby, G. L. Whiting, A. P. Alivisatos, *Adv. Funct. Mater.* **2003**, *13*, 73. b) J. Liu, T. Tanaka, K. Siluva, A. P. Alivisatos, J. M. J. Fréchet, *J. Am. Chem. Soc.* **2004**, *126*, 6550.
[10] a) B. Crone, A. Dodabalapur, A. Gelperin, L. Torsi, H. E. Katz, A. J. Lovinger, Z. Bao, *Appl. Phys. Lett.* **2001**, *78*, 2229. b) T. Someya, H. E. Katz, A. Gelperin, A. J. Lovinger, A. Dodabalapur, *Appl. Phys. Lett.* **2002**, *81*, 3079.
[11] a) C. Dekker, *Physics Today* **1999**, *52*, 22. b) Z. Yao, H. W. C. Postma, L. Balents, C. Dekker, *Nature* **1999**, *402*, 273. c) S. J. Tans, C. Dekker, *Nature* **2000**, *4*, 834.
[12] a) R. J. Kline, M. D. McGehee, E. N. Kadnikova, J. Liu, J. M. J. Fréchet, *Adv. Mater.* **2003**, *15*, 1519. b) B. S. Ong, Y. Wu, P. Liu, B. S. Gardner, *Adv. Mater.* **2005**, *17*, 1141.
[13] S. Berson, R. De Bettignies, S. Bailly, S. Guillerez, *Adv. Funct. Mater.* **2007**, *17*, 1377.
[14] A. Gesquière, P. Jonkheijm, F. J. M. Hoeben, A. P. H. J. Schenning, S. De Feyter, F. C. De Schryver, E. W. Meijer, *Nano Lett.* **2004**, *4*, 1175.
[15] L. Grill, K.-H. Rieder, F. Moresco, S. Stojkovic, A. Gourdon, C. Joachim, *Nano Lett.* **2005**, *5*, 859.
[16] V. Iancu, A. Deshpande, S.-W. Hla, *Nano Lett.* **2006**, *6*, 820.
[17] L. Scifo, M. Dubois, M. Brun, P. Rannou, S. Latil, A. Rubio, B. Grévin, *Nano Lett.* **2006**, *6*, 1711.
[18] M. Linares, L. Scifo, R. Demadrille, P. Brocorens, D. Beljonne, R. Lazzaroni, B. Grévin, *J. Phys. Chem. C* **2008**, *112*, 6850.
[19] Ph. Leclère, M. Surin, P. Brocorens, M. Cavallini, F. Biscarini, R. Lazzaroni, *Mater. Sci. Eng. Rep.* **2006**, *R55*, 1.
[20] M. Surin, Ph. Leclère, R. Lazzaroni, J. D. Yuen, G. Wang, D. Moses, A. J. Heeger, S. Cho, K. Lee, *J. Appl. Phys.* **2006**, *100*, 033712.
[21] D. Liu, S. De Feyter, M. Cotlet, U.-M. Wiesler, T. Weil, A. Herrmann, K. Muellen, F. C. De Schryver, *Macromolecules* **2003**, *36*, 8489.
[22] P. Samorì, M. Surin, V. Palermo, R. Lazzaroni, *Phys. Chem. Chem. Phys.* **2006**, *8*, 3927.
[23] S. Morita, R. Wiesendanger, E. Meyer, ''*Noncontact Atomic Force Microscopy. NanoScience and Technology*'', Springer, Berlin **2002**.
[24] F. J. Giessibl, *Rev. Mod. Phys.* **2003**, *75*, 949.
[25] S. Tanaka, H. Suzuki, T. Kamikado, S. Mashiko, *Nanotechnology* **2004**, *15*, S87.
[26] T. Dienel, C. Loppacher, S. C. B. Mannsfeld, R. Forker, T. Fritz, *Adv. Mater.* **2008**, *20*, 959.
[27] K. Sato, T. Sawaguchi, M. Sakata, K. Itaya, *Langmuir* **2007**, *23*, 12788.
[28] F. Lincker, N. Delbosc, S. Bailly, R. De Bettignies, M. Billon, A. Pron, R. Demadrille, *Adv. Funct. Mater.* **2008**, *18*, 3444.
[29] M. Surin, Ph, Leclère, S. De Feyter, M. M. S. Abdel-Mottaleb, F. C. De Schryver, O. Henze, W. J. Feast, R. Lazzaroni, *J. Phys. Chem. B* **2006**, *110*, 7898.
[30] M. Cavallini, P. Stoliar, J.-F. Moulin, M. Surin, Ph, Leclère, R. Lazzaroni, D. W. Breiby, J. W. Andreasen, M. M. Nielsen, P. Sonar, A. C. Grimsdale, K. Müllen, F. Biscarini, *Nano Lett.* **2005**, *5*, 2422.
[31] R. Demadrille, M. Firon, J. Leroy, P. Rannou, A. Pron, *Adv. Funct. Mater* **2005**, *15*, 1547.
[32] J. K. Herrema, J. Wildeman, F. van Bolhuis, G. Hadziioannou, *Synth. Met.* **1993**, *60*, 239.
[33] I. Horcas, R. Fernández, J. M. Gómez-Rodríguez, J. Colchero, J. Gómez-Herrero, A. M. Baro, *Rev. Sci. Instrum.* **2007**, *78*, 013705.
[34] N. L. Allinger, Y. H. Yuh, J. H. Lii, *J. Am. Chem. Soc.* **1989**, *111*, 8551.
[35] B. Y. Ma, J. H. Lii, N. L. Allinger, *J. Comput. Chem.* **2000**, *21*, 813.